JOURNAL OF Applied Polymer SCIENCE

Fabrication of Highly Isotactic Polypropylene Fibers to Substitute Asbestos in Reinforced Cement Composites and Analysis of the Fiber Formation Mechanism

Tetsuya Takahashi,[1] Yoko Tsurunaga,[1] Tetsuo Kondo[2]

[1]Faculty of Education, Shimane University, 1060 Nishikawatsu-cho, Matsue, Shimane 690-8504, Japan

[2]Faculty of Agriculture, Kyushu University, 6-10-1, Hakozaki, Higashi-ku, Fukuoka 812-8581, Japan

Correspondence to: T. Takahashi (E - mail: ttetsuya@edu.shimane-u.ac.jp)

ABSTRACT: Highly isotactic polypropylene (PP) is currently studied as a cement-reinforcement fiber that could potentially be substituted for asbestos because of its resistance to prolonged high-temperature curing. The higher the isotacticity of the PP fiber is, the higher the tensile modulus and breaking strength of the cured fiber are. The PP fiber that exhibits a isotacticity of 99.6% (XI) and draw ratio of 6.0 retains a tensile modulus of 4.23 GPa, even after high-temperature curing at 175°C for 5 h. PP fiber is cut into 6-mm lengths and dispersed throughout a cement mixture to prepare a reinforced cement composite. The mixture is cured in an autoclave at 175°C for 5 h. The Charpy impact strength and flexural strength of the obtained cement composite tends to increase with increasing PP isotacticity. © 2013 Wiley Periodicals, Inc. J. Appl. Polym. Sci. 130: 981–988, 2013

KEYWORDS: composites; crystallization; fibers; polyolefins; molding

Received 4 October 2012; accepted 24 February 2013; Published online 17 April 2013

DOI: 10.1002/app.39260

INTRODUCTION

When cement hydrates are cured at a high temperature of about 180°C, tobermorite with high crystallinity is formed very efficiently.[1] It is known that since this crystal has very high stiffness compared with the crystal formed under low temperatures, mechanical properties such as impact strength, flexural strength, and dimensional stability of reinforced cement composites increase. Because of the necessity for curing at a high temperature of about 180°C, asbestos, which has excellent heat resistance, was commonly used in the past as the reinforcing fiber for cement. However, the scattering of asbestos dust during building demolition has caused severe health problems, because of the carcinogenicity of asbestos, among other reasons.[2–5]

Consequently, acrylic, polyester, vinylon, and glass fibers are being examined as potential substitutes for asbestos.[6,7] However, since cement and aqueous cement solutions, in particular, are strongly alkaline and since these fibers do not exhibit sufficient alkaline resistance, they eventually deteriorate inside the cement. Polypropylene (PP) fibers, on the other hand, exhibit excellent resistance to alkaline environments but are not resistant to the prolonged high-temperature curing[8,9] required for producing reinforced cement composites. This is because PP fibers exhibit low heat resistance. Therefore, fibers that exhibit both excellent heat resistance and alkaline resistance comparable to that of asbestos were unavailable. However, with the progress of the Ziegler–Natta catalyst technology, the isotacticity of PP has been upgraded. In addition, metallocene catalysts[10] became applicable, which facilitated the synthesis of isotactic PP with high stereoregularity.[11] As a result, the crystallinity of PP increased, which improved the stiffness[12–14] and heat resistance[15,16] of PP.

In this study, fibers were produced using isotactic PP as a raw material because it exhibits excellent resistance to alkaline environments and higher isotacticity than does conventional PP. An autoclave curing test was then conducted to produce cement reinforcement fibers that exhibit excellent resistance to alkaline environments and endure prolonged exposure to high temperatures. We found that the shape of the PP fibers in the cement mixture was sufficiently retained even after curing for 5 h at 175°C, which exceeds the melting point of the fibers, and that the fibers had sufficiently reinforced the cement.

EXPERIMENTAL

Samples

Isotactic PP has a unique structure in which the methyl groups of the propylene side-chains are all oriented in the same direction and the propylene molecules are linked in a head-to-tail fashion. However, some of the methyl groups are oriented in the opposite direction, which decreases the stiffness and heat re-

Table I. Molecular Structure of Isotactic Polypropylene Samples

Sample	MFR (g/10 min)	M_w ($\times 10^4$)	M_w/M_n (-)	Isotacticity	
				XI (%)	IP (%)
PP-1	3.9	32.3	5.9	97.0	96.1
PP-2	3.5	32.8	5.7	98.1	97.6
PP-3	3.4	33.0	5.1	99.6	99.6

Additive formulation: Irg 1010/0.05%, Irgfos168/0.03%, Ca-st/0.08%.
M_w: Weight average molecular weight; M_n: Number average molecular weight.

sistance of PP. For this reason, three different isotactic PPs were used as samples in this study. The molecular structures of the isotactic PPs are listed in Table I. In compliance with the method described later in the section "Measurement Methods," the values of "XP" and "IP" indicating isotacticity were measured. The original PP sample was polymerized using a $MgCl_2$-supported catalyst (PP-3). For comparison, conventional low-isotacticity PP (PP-1, 2) polymerized with the Ziegler–Natta catalyst was also used. Three types of samples with the same melt flow rate (MFR) and weight-average molecular weight (M_w) and a large difference in isotacticity were used. The isotacticity of commercially available PP corresponds to PP-1. Further, 0.05% pentaerythritol tetrakis(3-(3,5-di-*tert*-butyl-4-hydroxyphenyl)propionate) (Irganox 1010, Ciba-Geigy), 0.03% tris(2,4-di-*tert*-butylphenyl)phosphite (Irgafos 168, Ciba-Geigy), and 0.08% calcium stearate were mixed (as additives) with all samples.

Fiber Production

Spinning Process. A 40 mm φ single screw extruder was used, and the heating temperature of the barrel was set with the following gradient: 200°C in the lower part of the hopper and 240°C in the die part. A 1.0 mm φ spinning nozzle with 20 holes and a length-to-diameter ratio (L/D) of 10 was used. The same melt-spinning conditions were set for all samples: spinning temperature, 240°C; discharge rate, 11.1 g min^{-1}; air gap, 50 mm; cooling water bath temperature, 30°C.[17]

Drawing Process. A drawing apparatus consisting of a hot-water bath (bath temperature: 100°C) was used, and strands discharged from melt-spinning were drawn based on an in-line system. The speed of the second roll was set at 100 m min^{-1}, and fibers with different draw ratios were prepared by changing the speed of the first roll.[17] The obtained fibers were cut into lengths of 6 mm. The fineness of the fiber after drawing was set at 55.6 dtex. The schematic diagram for the molding process of fibers is shown in Figure 1.

Preparation of Composites (Mortar Method). Ordinary Portland cement and silica sand were mixed in 1:1 ratio (weight ratio) for 1 min at 140 rpm in an agitator equipped with a stainless-steel paddle as a mechanical kneading unit. The obtained PP fibers (55.6 dtex, 6 mm Length) were then added in the proportion 2.0 parts (i.e., 2.0 parts per 100 rubber, phr) to 100 parts by weight of Portland cement and silica. The mixture was agitated for 1 min. Distilled water was added in the proportion 22.5 parts (22.5 phr) to 100 parts by weight of the dry mixture. The resulting mortar was agitated for an additional 1 min. When the flow value,[18] which indicates the fluidity of the mortar, was measured for the obtained mixture, all the samples exhibited extension diameters of ~155–163 mm, without any significant difference. The pH of the mixture was 11.5, which is strongly alkaline.

The obtained mortar was cast into a stainless-steel metal mold (250 mm long × 50 mm wide × 100 mm deep) and was well deaerated by flapping with a stainless-steel rod. After the surface was smoothed with a trowel, the mixture was left in a room controlled at 20°C and 60% humidity for 24 h. The composite was solidified by curing in an autoclave at 175°C for 5 h under 9.2 kg cm^{-2} of steam pressure. The conditions used for preparing the composites may change the physical properties of the composites. However, since the purpose of this study was to examine the effect of reinforcing fibers, the preparation conditions were maintained constant. The volume fraction of the PP fibers in the cement composites was about 6.4 vol %, assuming the density of Portland cement and silica sand to be 3.15 and 2.65 g cm^{-3}, respectively. The schematic of the reinforced cement composites is shown in Figure 2.

Measurement Methods

Isotacticity of PP. As a rough standard of the isotacticity of PP, the insoluble quantity of PP in xylene was measured. PP pellets were completely dissolved in xylene at 135°C. The mixture was

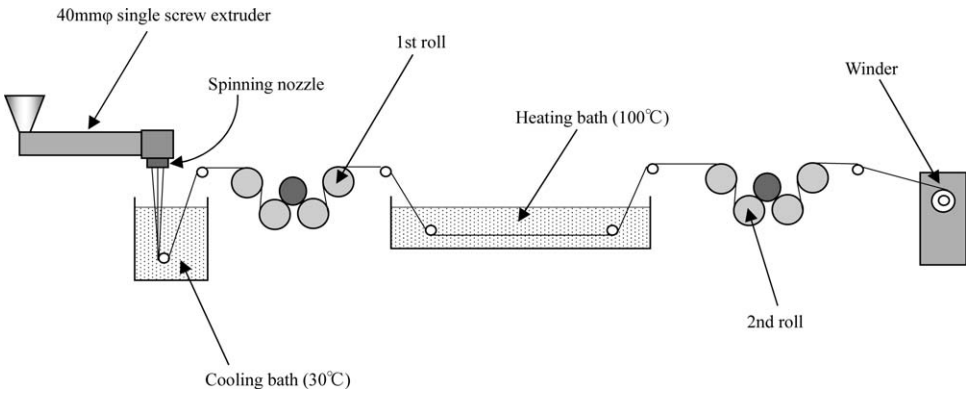

Figure 1. Schematic representation of fiber spinning process.

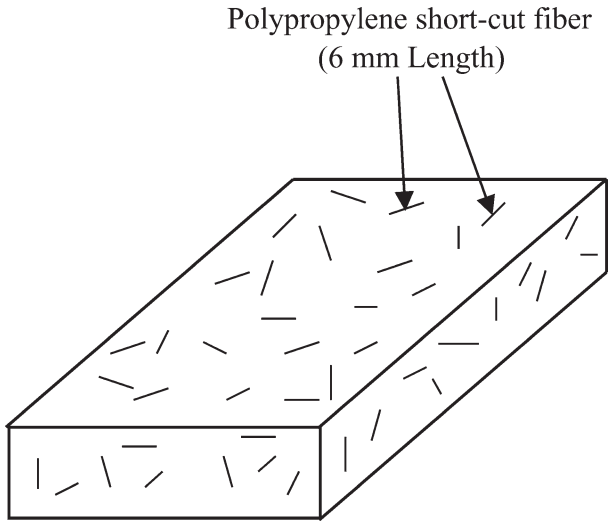

Figure 2. A schematic representation of reinforced cement composites containing short-cut PP fiber (6 mm in length).

then cooled to 25°C, and the ratio of the weight of the precipitate to the total weight of the polymer was measured at this stage. This ratio (i.e., insoluble part during 25°C xylene extraction) is expressed as XI hereafter.

From the peak intensity in ^{13}C-NMR spectra, various forms of formation on the isotacticity of PP can be obtained. ^{13}C-NMR spectra were generated for the PP dissolved in 25% (w/v) 1,2,4-trichlorobenzene at 140°C, using the JNM-GSX400 spectrometer produced by JEOL. However, in the case of pentads (mmmm), significant overlapping with other peaks was observed. Calculations were performed using a two-site model.[19] The fraction of the isotactic pentad (mmmm) of the methyl groups in the polymer molecule chains was calculated based on Zambelli et al.'s article.[20] This value is denoted by IP hereinafter.

Mechanical Properties of Fiber. Using Tensilon UTM-III-500 manufactured by Orientec Co., a tension test was carried out under the following conditions: thermostatic chamber temperature (23°C), sample length (100 mm), and tension rate (100 mm min^{-1}; equivalent to 100% min^{-1} of strain rate). The breaking strength of the fibers was obtained by dividing the load at the fracture point by the cross-section area of the fiber. The breaking elongation of the fibers was obtained by dividing the elongation at the breaking point by the sample length. A tangent line was drawn on the rising part of the stress–strain curve in the tension test, and then, the tensile modulus was calculated from its slope. The measurement was repeated 10 times, and the average value was obtained. In addition, error bars indicating the maximum and minimum were added to the graph.

Endothermic Behavior of Melting PP. Differential scanning calorimetry was conducted using a DSC-200 calorimeter produced by Seiko Instruments. Approximately 2.5 mg of finely cut fiber was packed into an aluminum pan placed in a nitrogen gas atmosphere, and the temperature was raised and lowered in the range 50–230°C at the rate of 10°C min^{-1}.

The melt onset temperature (T_{ms1}) and melting peak temperature (T_{mp1}) were measured from the endothermic melting curve generated by melting the fiber during the initial heating. The crystallization peak temperature (T_{cp}) was measured from the crystallization exothermic curve generated during cooling. Heating was repeated, and the melt onset temperature (T_{ms2}) and melting peak temperature (T_{mp2}) were measured. The melt endotherm (ΔH) was obtained from the area of the melt endothermic curve generated during heating, and weight crystallinities (X_{c1}, X_{c2}) were calculated using the amount of energy per gram required to melt the PP crystal (163 J g^{-1}),[21] as reported in the literature. The temperature and melt endotherms were corrected using indium (melting point: 156.4°C) as a calibration standard.[22,23]

Fluidizing Property of Mortar. The mortar slurry was packed into a conical stainless-steel cup and placed on a table. After the table was vertically vibrated 15 times at 1 vibration s^{-1}, the extension diameter of the mixture was measured. After two tests, the average was used as the flow value.[18]

Flexural Strength of Reinforced Cement Composite. The flexural strength of the sample after autoclave curing was tested based on JIS A 1408, and a stress–strain curve was obtained for the sample under a given load. When the load that increased nearly linearly started to drop, increased again, and reached the maximum, its value (W kg) was read from the stress–strain curve. From the load (W kg), span (L cm), width of the sample (b cm), and thickness of the sample (d cm), the flexural strength was obtained using the following equation.

$$\text{flexural strength (kgf cm}^{-2}) = 3 \cdot W \cdot L/2 \cdot b \cdot d^2$$

Charpy Impact Strength of Reinforced Cement Composite. The cured reinforced cement composite was cut to a width of 12 mm with a diamond cutter, and its surface was smoothed by grinding. Ten samples (70 mm long × 15 mm wide × 12 mm thick) were cut from the composite. The Charpy impact strength was measured at 5 kgf·cm of hammer energy on the basis of the JIS-B-7722 standard. The error bars indicate the maximum and minimum values.

RESULTS AND DISCUSSION

Drawability and Mechanical Properties of Fiber

Strands after melt-spinning were treated by in-line one-step drawing in a hot-water bath heated to 100°C. The draw ratio when whitening occurred in the fibers was 8.0, 8.5, and 9.0 times, starting from the sample with the highest isotacticity. In addition, the draw ratio when breaking occurred was 9.0, 11.0, and 11.0 times, starting from the sample with the highest isotacticity. This means that as the isotacticity of the sample increases, the drawability during manufacturing tends to decrease. This result suggests that a pre-drawn fiber produced from highly isotactic PP resists the unfolding of lamellar crystals because of its high crystallinity.

The relation between the ultimate breaking strength and the draw ratio of the obtained fibers is shown in Figure 3(a). The breaking strength of the PP fibers in all the samples increased linearly with increasing draw ratio. Moreover, isotacticity had

Applied Polymer SCIENCE

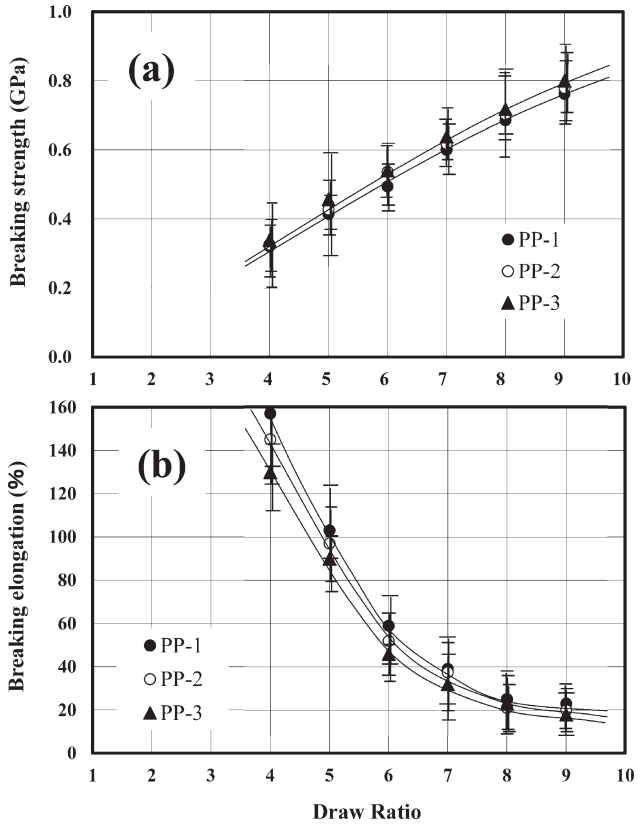

Figure 3. Tensile properties of PP fibers versus draw ratio for different isotacticities. (a) Breaking strength (b) Breaking elongation.

minimal effect on the breaking strength, which tended to increase with increasing isotacticity. The relation between the breaking elongation and draw ratio of the fibers is shown in Figure 3(b). The result shows that although the difference was negligible when the draw ratio was 7.0 or more, the breaking elongation decreased with increasing PP isotacticity when the draw ratio was 6.0 or less. This fact suggests that PP prepared from the sample with higher isotacticity was more resistant to structural change, which corresponds to drawability during manufacturing.

The relation between the tensile modulus and draw ratio of the fibers is shown in Figure 4. All the PP fibers showed a linear increase in the tensile modulus when the draw ratio was in the range between 4 and 7. However, in the range between 8 and 9, the slope of the line tended to decrease. In addition, the tensile

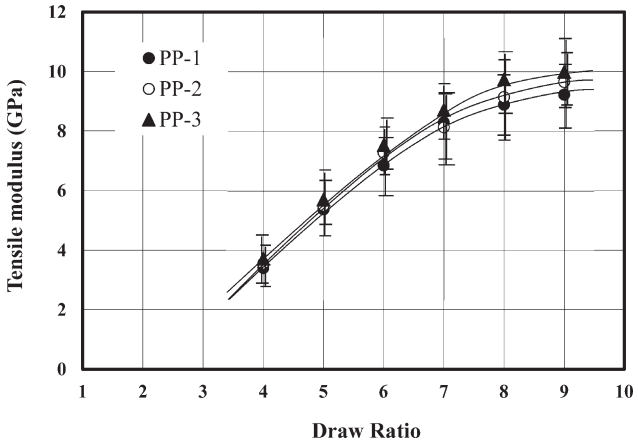

Figure 4. Tensile modulus of PP fibers versus draw ratio for different isotacticities.

modulus of the fibers increased as the isotacticity of PP increased. This result suggests that the highly isotactic PP fiber exhibited high rigidity because of its high crystallinity. In general, the higher the tensile modulus of the fiber, the better is the reinforcement it will provide for cement. In other words, highly isotactic PP fibers provide better cement reinforcement.

Thermal Properties of Fiber

The endothermic melting behavior during heating was determined by differential scanning calorimetry (DSC) for the fibers produced from different isotactic PPs with a draw ratio of 6.0. The results are listed in Table II. During the first heating, when the melt endothermic behavior is derived from the fiber itself, PP-3, the most highly isotactic sample exhibited the highest melting peak temperature (T_{mp1}), reaching 169.1°C. PP-1 and PP-2, on the other hand, exhibited lower melting peak temperatures at 164.9 and 164.6°C, respectively. This result indicates that the fibers exhibiting isotacticities (XIs) of 98.1 and 99.1% exhibited a difference of ~5 K (°C) in their melting peak temperatures. Similarly, the melt onset temperature (T_{ms1}) was high when the isotacticity was high. In general, when XI exceeds 99%, a very high melting point can be obtained.

During the second heating (i.e., re-melting), the melt onset temperature (T_{ms2}) and melting peak temperature (T_{mp2}) were examined. Since the crystalline orientation of the fibers decreased because of heat, both T_{ms2} and T_{mp2} were lower than their counterparts during the first heating. However, even during the second heating, the highly isotactic PP-3 retained a

Table II. Thermal Properties of PP Fiber for Different Isotacticities (Draw Ratio is 6.0)

			1st heating			2nd heating			1st cooling
Sample	Isotacticity XI (%)	Draw ratio	Tms_1 (°C)	Tmp_1 (°C)	Xc_1 (%)	Tms_2 (°C)	Tmp_2 (°C)	Xc_2 (%)	Tcp (°C)
PP-1	97.0	6.0	149.2	164.6	67.2	140.8	160.3 (146.0)[a]	64.3	115.0
PP-2	98.1	6.0	148.1	164.9	67.4	142.5	161.1 (146.6)[a]	63.6	115.4
PP-3	99.6	6.0	153.2	169.1	72.5	156.6	165.4	70.6	119.7

[a] Sub-peak.

Table III. Thermal Properties of High-Isotacticity PP Fiber for Different Draw Ratios

			1st heating			2nd heating			1st cooling
Sample	Isotacticity XI (%)	Draw ratio	Tms_1 (°C)	Tmp_1 (°C)	Xc_1 (%)	Tms_2 (°C)	Tmp_2 (°C)	Xc_2 (%)	Tcp (°C)
PP-3	99.6	4.0	155.2	168.6 (159.1)[a]	70.2	154.9	164.8	68.0	117.4
PP-3	99.6	6.0	153.2	169.1	72.5	156.6	165.4	70.6	119.7
PP-3	99.6	8.0	154.8	171.0	74.1	152.8	164.7	68.6	117.0

[a] Sub-peak.

comparatively high T_{mp2} of 165.4°C. Even the second melt onset temperature (T_{ms2}) was high for the highly isotactic PP.

In the next step, the crystallization peak temperature (T_{cp}) was examined during cooling. PP-3, which exhibited the highest isotacticity, also exhibited a higher crystallization peak temperature than did both PP-1 and PP-2 during cooling. This result suggests that PP-3 probably retained the crystal nuclei even after exposure to a temperature of 230°C, which may be because of its superior isotacticity.

Fibers with draw ratios in the range 4.0–8.0 were then prepared using PP-3, and their melt endothermic behavior was examined to determine whether their crystallinity could be maintained at high temperatures. The results are listed in Table III. The melting peak temperature (T_{mp1}) during the first heating was higher in proportion to the draw ratio, reaching 171.0°C, for the fiber produced with a draw ratio of 8.0. In other words, a fiber with a high melting point exceeding 170°C could be achieved using PP-3 fiber as the starting material. During the second heating, on the other hand, all fibers exhibited melting peak temperatures (T_{mp2}) of ~165°C. This result suggests that the crystalline orientation had decreased during melting in the first heating, which nullified the enhanced crystallinity due to the draw ratio. In Table III, although the samples exhibited improved isotacticity during the second heating, crystallinity enhancement due to the draw ratio was not observed. This tendency was the same for the crystallization peak temperature (T_{cp}) during cooling, and the enhanced crystallinity due to the draw ratio was negligible.

The crystallinity of fibers obtained for various melt endotherms was then examined, and the results are listed in Tables II and III. The crystallinity during the first heating (X_{c1}), which is derived from the fiber itself, increased with increasing isotacticity or draw ratio. This result indicates that the PP crystal becomes more complete with increasing isotacticity and that the crystallinity increases even after fiber formation. In addition, the high draw ratio tended to result in higher crystallinity.

During the second heating, the crystallinity had clearly decreased as compared to that (X_{c1}) obtained during the first heating. However, the highly isotactic PP-3 still exhibited a comparatively high crystallinity of 70.6% (Table II). In addition, the crystallinity of PP-3 during the second heating (X_{c2}) was unaffected by the draw ratio (Table III).

Effect of Autoclave Curing on PP Fiber

Prior to the autoclave curing test of the cement composites embedded with short fibers, autoclave curing using the composites embedded with fibers without cutting was conducted. In this experiment, PP fibers with a draw ratio of 6.0 and different isotacticities were used. The cured reinforced cement composite was then cut in the direction of the fiber. The fiber was removed, and its external appearance was inspected. The PP fiber embedded in the cement composite maintained almost the original shape during high-temperature curing. The mechanical properties of the cured fiber were then measured.

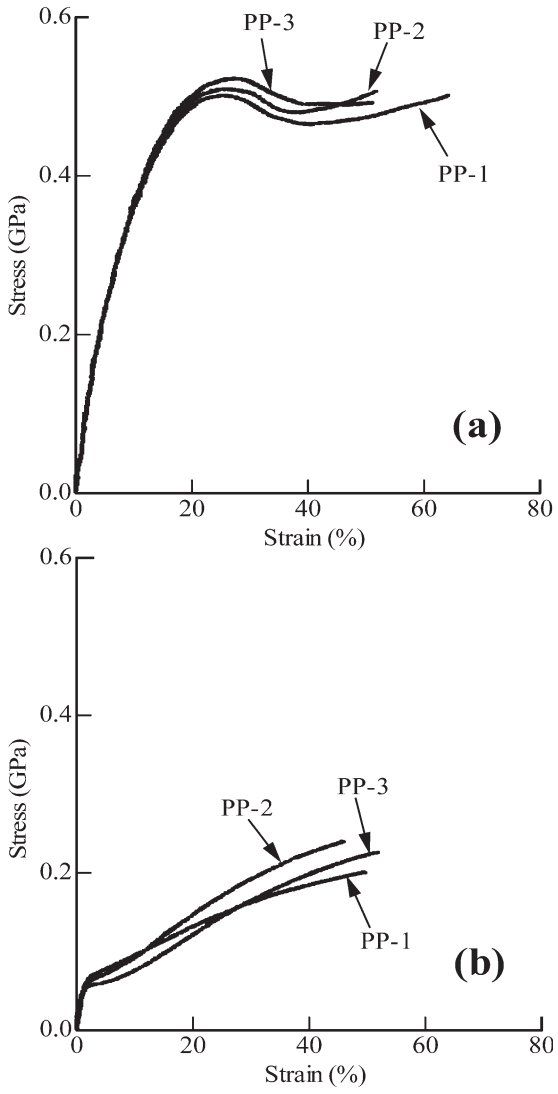

Figure 5. Stress–strain curves of PP fibers for different isotacticities at a strain rate of 100% min^{-1} (draw ratio is 6.0). (a) Before autoclave curing and (b) after autoclave curing at 175°C for 5 h.

Applied Polymer SCIENCE

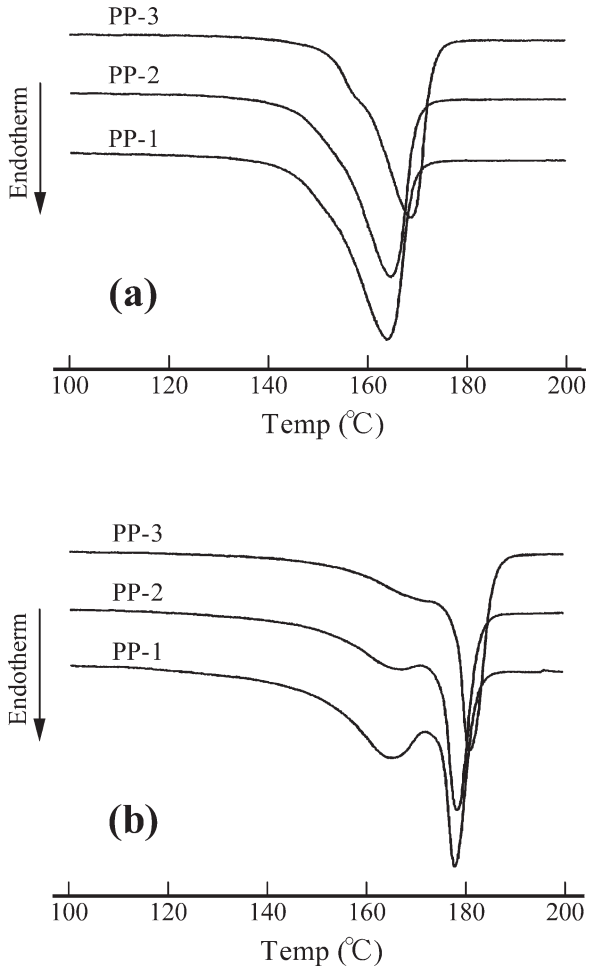

Figure 6. DSC curves of PP fibers for different isotacticities in the heating process for 100°C to 200°C at a rate of 10°C min^{-1} before autoclave curing (draw ratio is 6.0). (a) Before autoclave curing and (b) after autoclave curing at 175°C for 5 h.

A tension test was conducted for the fibers with a draw ratio of 6.0 that were prepared using PP-1, PP-2, and PP-3 with different isotacticities. The stress-strain curve of the fiber before curing is shown in Figure 5(a), and that after curing is shown in Figure 5(b). The result showed that the tensile stress of all the fibers deteriorated after curing. In addition, the yield point of the stress–strain curve that appeared at 25–27% before curing disappeared after curing. In spite of this, even after curing at 175°C for 5 h, the stress exceeding 0.2 GPa was still maintained.

The tensile modulus of the cured fiber increased with increasing isotacticity. In general, fibers that exhibited high isotacticity retained their high tensile modulus during heating at 175°C for 5 h. In particular, the PP-3 fiber retained a tensile modulus of 4.23 GPa.

The endothermic melt behavior of the cured fibers was then measured using DSC. The melting endothermic peak of the PP fibers before curing is shown in Figure 6(a), and that after curing is shown in Figure 6(b). The melting endothermic peak of the fiber of PP-3 with the highest isotacticity appeared at the highest temperature. After curing, all fibers shifted the melting endothermic peaks to the higher-temperature side. Even after curing, the melting endothermic peak of the PP with the highest isotacticity shifted further to the higher-temperature side. On the other hand, in the fibers with low isotacticity, such as PP-1 and PP-2, the melting endothermic peaks on the lower-temperature side that had appeared before curing reappeared, revealing two peaks. The results are listed in Table IV. All cured fibers exhibited higher melting peak temperatures than did their uncured counterparts. The melting peak temperature of the cured fibers was higher for the more highly isotactic PPs, and heating during curing increased their thermal stability. It should be noted that although the samples were cured for 5 h at 175°C, the melting peak temperature of the fibers further increased because the curing temperature exceeded the melting point of the fibers. This result suggests that deformation, as with thermal shrinkage, was restricted because the fiber was embedded in the cement and that the crystallization of the fiber further increased because of heat treatment during curing. It has been demonstrated that the PP fiber did not melt during curing and that curing actually increased the melting peak temperature of the fiber.

Because PP-3 exhibited the highest isotacticity, the PP-3-based fibers produced with different draw ratios were then cured in the autoclave at 175°C for 5 h. The mechanical properties of the fibers before and after curing are listed in Table V. Through the curing at 175°C for 5 h, the tensile modulus of PP fiber decreased, regardless of the draw ratio. However, the fiber with a high draw ratio of 8.0 maintained a relatively high tensile modulus of 4.06 GPa even after curing. Furthermore, the melt endothermic behaviors of the PP-3-based fibers produced with different draw ratios were measured using DSC, and the results

Table IV. Change in Mechanical Properties of PP Fibers for Different Isotacticities by Autoclave Curing (175°C × 5 h)

Sample	Draw ratio	Autoclave curing	Breaking strength (GPa)	Breaking elongation (%)	Tensile modulus (GPa)	Tmp_1[a] (°C)
PP-1	6.0	Before	0.49	80	6.86	164.6
		After	0.24	45	2.79	176.5
PP-2	6.0	Before	0.54	52	7.28	164.9
		After	0.30	40	3.98	176.3
PP-3	6.0	Before	0.54	46	7.54	169.1
		After	0.31	48	4.23	179.6

[a] Tmp_1: Melting peak temperature.

Table V. Change in Mechanical Properties of PP Fibers for Different Draw Ratios by Autoclave Curing (175°C × 5 h)

Sample	Draw ratio	Autoclave curing	Breaking strength (GPa)	Breaking elongation (%)	Tensile modulus (GPa)	Tmp_1[a] (°C)
PP-3	4.0	Before	0.34	130	3.73	168.6
		After	0.12	55	0.93	168.1
PP-3	6.0	Before	0.54	46	7.54	169.1
		After	0.31	48	4.23	179.6
PP-3	8.0	Before	0.72	23	9.74	171.0
		After	0.39	32	4.06	178.4

[a] Tmp_1: Melting peak temperature.

are listed in Table V. All the cured fibers exhibited higher melting peak temperatures than did their uncured counterparts. Moreover, the melting peak temperature of the cured fibers tended to increase with increasing draw ratio. When the draw ratio exceeded 6.0, the melting peak temperature increased to ~178.4–179.6°C.

Factors Affecting Impact Strength of Reinforced Cement Composites

The cement composites were embedded with 6-mm-long PP fibers and subjected to autoclave curing, and subsequently, their flexural strength was measured. Then, the effect of the tensile modulus of the fibers after curing (Tables IV and V) on the flexural strength of the cement composites was examined [Figure 7(a)]. The result showed that the flexural strength increased when the tensile modulus of the fibers after curing exceeded 3.7 GPa. In other words, fibers with high isotacticity and high draw ratio showed a relatively high tensile modulus and increased the flexural strength of the cement composites. In other words, the tensile modulus of the fibers after curing controlled the flexural strength of the cement composites.

The melting peak temperature of the fibers had a similar effect as did the tensile modulus on the flexural strength of the cement composites [Figure 7(b)]. The thermal stability of the cured fibers had a marked influence on the flexural strength of the cement composites: the flexural strength increased with the melting peak temperature.

In the following step, the Charpy impact strength of the cured cement composites was measured, and its dependence on the tensile modulus of the fibers (Tables IV and V) was investigated [Figure 8(a)]. As a result, the tensile modulus of the fibers after

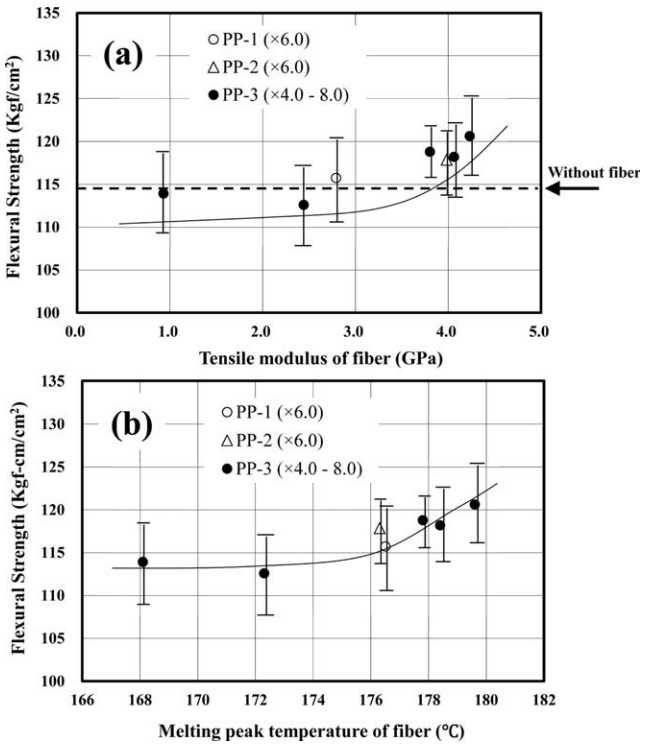

Figure 7. Relationship between flexural strength and properties of PP fiber in reinforced cement composites after autoclave curing. Fiber: 5.6 dtex, 6 mm in length (mixing at a ratio of 2.0 phr); Autoclave curing at 175°C for 5 h (a) versus tensile modulus and (b) versus melting peak temperature.

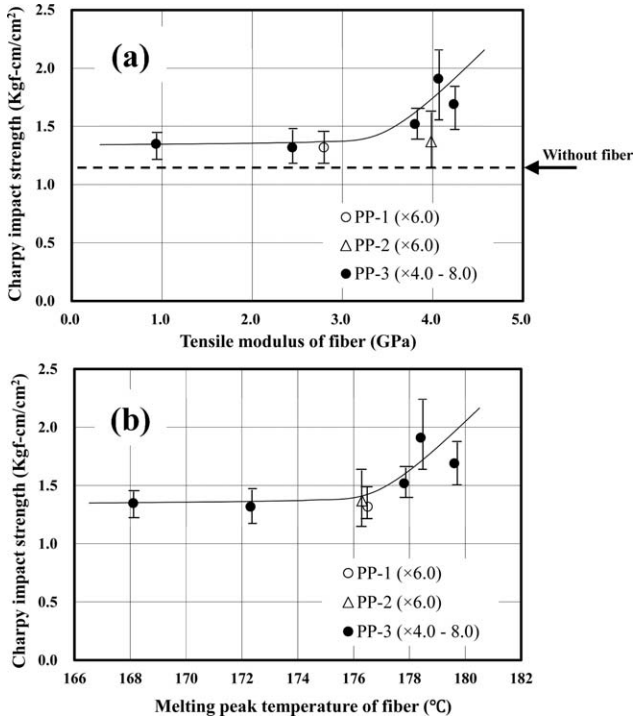

Figure 8. Relationship between Charpy impact strength and properties of PP fiber in reinforced cement composites after autoclave curing. Fiber: 5.6 dtex, 6 mm in length (mixing at a ratio of 2.0 phr); Autoclave curing at 175°C for 5 h (a) versus tensile modulus and (b) versus melting peak temperature.

curing had the similar effect on the Charpy impact strength of cement composites, to the effect on the flexural strength of cement composites shown in Figure 7(a). When the tensile modulus of the fibers was high, the Charpy impact strength of the cement composites, too, was high. When the flexural strength of the fibers exceeded 3.7 GPa after curing, the Charpy impact strength increased, similar to the flexural strength of the cement composites. Thus, it can be said that the tensile modulus of the cured fibers controls the Charpy impact strength of the cement composites.

In addition, the effect of the melting peak temperature of the cured fibers (Tables IV and V) on the Charpy impact strength of the cement composites was examined [Figure 8(b)]. As a result, the melting peak temperature of the fibers after curing has similar effect on the Charpy impact strength of cement composites, to the effect on the flexural strength of cement composites. The impact strength increased in direct proportion to the melting peak temperature. The volume fraction of the PP fibers in the cement composites was about 6.4 vol %. It was found that even under such volume fraction, it sufficiently contributes to improvement in the flexural strength and Charpy impact strength of cement composites.

After the Charpy impact test, a large number of fibers were seen to protrude from the fracture surface of the composites, indicating insufficient contact between the cement matrix and the fibers. Surface treatment or any other suitable method can be applied to the PP fibers so that the fiber–cement affinity and the reinforcing effect of the fiber on the cement composites are improved. The results suggest that fibers produced using highly drawn and isotactic PP have great potential for use in cement reinforcement because of their excellent heat resistance during prolonged high-temperature curing.

PP has better chemical resistance as compared to other synthetic fibers such as vinylon, polyester, and acryl, but its heat resistance is low, i.e., it cannot endure autoclave curing. This study clarified that PP fibers with high isotacticity can endure autoclave curing. The fibers obtained from PP with high stereoregularity may find widespread application as construction materials, that is, as floor and wall materials for houses and super-high-rise buildings.

CONCLUSIONS

Highly isotactic PP fibers were tested for application in cement reinforcement because of their excellent alkaline resistance and stability against prolonged exposure to high temperatures during curing. The PP fibers were embedded in the cement, and the reinforced cement composites were cured in an autoclave at 175°C for 5 h. The effects of the fiber isotacticity and high-temperature curing on the Charpy impact strength of the reinforced cement composites were examined. The results are as follows:

1. As the isotacticity of the PP fibers increased, the mechanical properties of the fibers produced using the same draw ratio also increased. In addition, as the isotacticity increased, the melting peak temperature and crystallinity of the PP fibers increased.
2. PP fibers were embedded into reinforced cement composites and cured in an autoclave at 175°C for 5 h. The mechanical properties and melting peak temperatures of the fibers were measured. The results show that the tensile modulus and melting peak temperatures of the cured fibers increased with increasing isotacticity or draw ratio. In particular, the fiber that exhibited 99.6% isotacticity (XI) and a draw ratio of 8.0 exhibited a melting peak temperature of 178.4°C, even after high-temperature curing.
3. Cement mixtures containing 6-mm-long PP fibers were cured at 175°C for 5 h to prepare reinforced cement composites. The Charpy impact strength of the obtained reinforced cement composites increased with increasing PP fiber isotacticity. These results suggest that cement-reinforcement fibers produced using highly drawn and isotactic PP are sufficiently resistant to prolonged high-temperature curing.

REFERENCES

1. Chan, C. F.; Sakiyama, M.; Mitsuda, T. *Cem. Concr. Res.* **1978**, *8*, 1.
2. Hirano, S. *Jpn. J. Thromb. Hemost.* **2006**, *17*, 74.
3. Kumagai, S.; Kurumatani, N. *J. Occup. Health* **2007**, *49*, 77.
4. Bianchi, C.; Bianchi, T. *Ind. Health* **2007**, *45*, 379.
5. Hessel, P. A. *Indoor Built Environ.* **1999**, *8*, 127.
6. Nishiyama, S. *Jpn. Res. Assoc. Text End-Uses* **2005**, *46*, 772.
7. Woods, D. M. *Constr. Build Mater.* **1990**, *4*, 3, 127–131.
8. Funamoto, K.; Umeda, T.; Koga, T. *Cem. Sci. Concr. Technol.* **2006**, *59*, 427.
9. Ramamurthy, K.; Narayanan, N. *Mater. Struct.* **2000**, *33*, 243.
10. Sinn, H.; Kaminsky, W.; Vollmer, H. J.; Woldt, R. *Angew. Chem. Int. Ed. Engl.* **1980**, *19*, 390.
11. Brintzinger, H. H.; Fischer, D.; Mulhaupt, R.; Rieger, B.; Waymouth, R. M. *Angew. Chem., Int. Ed. Engl.* **1995**, *34*, 1143.
12. Gahleitner, M.; Neissl, W.; Pitkaenen, P.; Jaeaeskelaeinen, P.; Malm, B. *Kunstst. Plast. Eur.* **2001**, *91*, 20.
13. Phillips, R. A. *Polyolefins* **1999**, *11*, 793.
14. Edward P. M. Jr Ed. Polypropylene Handbook – Polymerization, Characterization, Properties, Processing, Applications; Hanser Publishers, New York, **1996**; p 241.
15. Matsuda, M.; Nomura, T.; Iwai, H. *SAE Technical Paper* **1998**, *982410*, 1.
16. Fujiyama, M.; Kitajima, Y.; Inata, H. *J. Appl. Polym. Sci.* **2002**, *84*, 2142.
17. Takahashi, T.; Tanaka, T.; Kamei, R.; Okui, N.; Takahiro, M.; Umemoto, S.; Sakai, T. *Sen'i Gakkaishi*, **1988**, *44*, 165.
18. JIS R5201, Physical Testing Methods for Cement.
19. Zhu, S.; Yang, X.; Chujo, R. *Polym. J.* **1989**, *12*, 859.
20. Zambelli, A.; Locatelli, P.; Provasoli, A.; Ferro, D. R. *Macromolecules* **1980**, *13*, 267.
21. Encyclopedia of Polymer Science and Engineering; Wiley, **1984**; Vol. *4*, p 482.
22. Geert, V. P.; Matho, T.; Vincent B. F. *Thermochim. Acta* **2006**, *446*, 41.
23. Claudy, P.; Commercon, J. C.; Letoffe, J. M. *Thermochim. Acta* **1983**, *68*, 317.